A Study of the Anomeric Effect on an Electronic Scale: The Electron Density of 1,4-Dioxane and *trans*-2,5-Dichloro-1,4-dioxane

T. Koritsánszky,[†] M. K. Strumpel,[‡] J. Buschmann,[‡] P. Luger,*[,‡] N. K. Hansen,[§] and V. Pichon-Pesme[§]

Contribution from the Central Research Institute for Chemistry of the Hungarian Academy of Sciences, Budapest, Hungary, Institute for Crystallography, Free University of Berlin, D-1000 Berlin 33, Germany, and Laboratory of Mineralogy, Crystallography and Infrared Physics, University of Nancy I, France. *Received March 21, 1991*

Abstract: The low-temperature molecular structure and electron density (ED) distribution of dioxane (DIOX) and *trans*-2,5-dichloro-1,4-dioxane (DICLOX) were determined near 100 K from X-ray data. The geometry of the chlorinated molecule is in accord with the predictions of the anomeric effect. Electron deformation density (EDD) maps were calculated by Fourier and multipole expansion techniques and compared to those obtained by ab initio Hartree–Fock methods. The multipole model charge distribution of DIOX determined from experimental data was taken as a reference state, relative to which the ED of the substituted ring was analyzed. These fragment deformation density (FDD) maps show quadrupolar deformations which are strictly localized on the O, Cl, and anomeric C atoms. The highly correlated orientation of the lobes at these atomic sites may indicate that the observed charge rearrangement is due to three-center interactions, although these local features of the FDD cannot be interpreted on the basis of a specific molecular orbital coupling such as the $n_\pi(O)-\sigma^*(C-Cl)$ overlap. The quadrupoles at the O and at the Cl atoms are situated in the C–O–C plane and parallel to it, respectively. This may imply that the σ lone pair of the oxygen and the π lone pairs of the Cl atom are also involved in the bonding.

Introduction

The anomeric effect[1] plays an important role in carbohydrate chemistry by influencing the conformation of sugar rings. In contrast to steric requirements that bulky substituents on a flexible pyranose ring should stay clear of each other and of the ring by taking up equatorial conformation, the anomeric effect guides electronegative substituents into the more crowded axial setting (see Figure 1).

The anomeric effect is observed when two electronegative substituents are attached to an sp^3-hybridized carbon atom. This occurs for a pyranose ring, or for a dioxane ring, when for instance a halogen atom (X) is attached to a carbon atom next to the ring oxygen. While in crystalline *trans*-1,4-dichlorocyclohexane only equatorial chlorine atoms are found,[2] all trans-dihalogenated dioxanes investigated by C. Romers, C. Altona, H. R. Buys, and E. Havinga[3] were in the diaxial conformation. A further manifestation of the anomeric effect is the lengthening of the C–X and the shortening of the C–O bond. An equatorial carbon to chlorine bond was observed in *cis*-2,3-dichloro-1,4-dioxane, where the chair conformation allows only one axial C–Cl bond. The length of this equatorial bond, 1.782 (7) Å, is within the range valid for paraffins, while the axial bond in the same compound 1.819 (9) Å, is comparable to other axial anomeric C–Cl bonds. Luger et al.[4] reported 1.859 (4) and 1.754 (7) Å, respectively, for an axial and an equatorial anomeric C–Cl bond on substituted xylopyranoses. For the corresponding fluoro compounds, the axial C–F bond is 1.392 (5) and the equatorial bond 1.367 (4)[5] Å.

The anomeric effect in an O–C–X fragment is usually interpreted in terms of localized MO's. It is stated that charge back-donation from the O to the C atom occurs via nonbonding–antibonding ($n-\sigma^*$) orbital interaction in order to compensate for the polarity of the C–X bond.[6] On an energetic basis, the less localized $n_\pi(O)$ is more likely to be involved in orbital coupling than the more strongly bound $n_\sigma(O)$. This argument dictates the preference of the axial $n_\pi(O)-\sigma^*(C-X)$ coupling over the equatorial $n_\sigma(O)-\sigma^*(C-X)$ interaction. The change in bond densities due to MO coupling might not be observable either by experimental or by theoretical methods, but the interaction should manifest itself as charge transfer from the terminal atoms to the central carbon, accompanied by a charge rearrangement in the nonbonded areas.

A combined X-ray and neutron charge density study on β-DL-arabinose[7] showed significant asymmetry in the nonbonded regions of the oxygen atoms participating in the MO coupling. On the difference Fourier maps more pronounced peaks were obtained for the π than for σ lone pairs. In order to find more details on the anomeric effect, the low-temperature crystal structure of DICLOX with two equivalent anomeric centers was reinvestigated, and for comparison, the ED of the unsubstituted dioxane was also studied. Both compounds crystallize in centrosymmetric space groups; thus, they are especially suitable for ED investigations.

The structure of two crystalline phases of DIOX was investigated by J. Buschmann, E. Müller, and P. Luger.[8] For phase I at 279 K 500 and for phase II at 153 K 627 observed reflections were measured. The structure of *trans*-2,5-dichloro-1,4-dioxane was first determined by C. Altona, C. Knobler, and C. Romers[9] at 148 K with 653 reflections.

Experimental Section

Dioxane. Another X-ray data set was collected for phase II of DIOX at 106 K. This phase exists below 278 K, phase I from 278 to 285 K. Since DIOX is a liquid at room temperature, a single crystal was grown in a glass capillary by cooling. The method is described by J. Buschmann et al.[8] Cooling was provided by a nitrogen gas stream device.[10] Crystal and experimental data are listed in Table I. Since the crystallized material extends beyond a length that can constantly be bathed in radiation, the reflection intensities were corrected for the changing crystal volume hit by the X-ray beam.[11]

[†] Central Research Institute for Chemistry of the Hungarian Academy of Sciences.
[‡] Free University of Berlin.

(1) Kirby, A. J. The Anomeric Effect and Related Stereoelectronic Effects at Oxygen. *Mol. Struct.* **1983**, *15*.
(2) Hassel, O.; Vihovde, E. H. *Acta Chem. Scand.* **1953**, *7*, 1164.
(3) Romers, C.; Altona, C.; Buys, H. R.; Havinga, E. *Top. Stereochem.* **1969**, *4*, 73–77.
(4) Luger, P.; Kothe, G.; Paulsen, H. *Chem. Ber.* **1976**, *109*, 1850–1855.
(5) Kothe, G.; Luger, P.; Paulsen, H. *Acta Crystallogr.* **1979**, *B35*, 2079–2087.
(6) Altona, C. Doctoral Dissertation, University of Leiden, 1964.
(7) Longchambon, P. F.; Gillier-Panduraud, H.; Wiest, R.; Rees, B.; Mitschler, A.; Feld, R.; Lehmann, M.; Becker, P. *Acta Crystallogr.* **1985**, *B41*, 47–56.
(8) Buschmann, J.; Müller, E.; Luger, P. *Acta Crystallogr.* **1986**, *C42*, 873–876, 1274.
(9) Altona, C.; Knobler, C.; Romers, C. *Acta Crystallogr.* **1963**, *16*, 1217.
(10) Dietrich, H.; Dierks, H. *Messtechnik (Braunschweig)* **1970**, *78*, 184–186.

0002-7863/91/1513-9148$02.50/0

Table I. Crystal and Experimental X-ray Data for 1,4-Dioxane and *trans*-2,5-Dichloro-1,4-dioxane

	1,4-dioxane	*trans*-2,5-dichloro-1,4-dioxane
formula	$C_4H_8O_2$	$C_4H_6O_2Cl_2$
formula weight (g/mol)	88.104	156.99
space group	$P2_1/n$	$P\bar{1}$
formula units per cell (Z)	2	1
cell dimensions based on the orientation reflections		
a (Å)	5.715 (2)	4.504 (2)
b	6.458 (2)	5.419 (2)
c	6.131 (2)	6.586 (2)
α (deg)	90.0	85.50 (2)
β	99.89 (3)	103.83 (3)
γ	90.0	106.55 (3)
cell volume (Å^3)	222.9 (2)	149.6 (2)
linear absorption coeff (μ (cm^{-1}))	0.962	9.87
density (g/cm^3)	1.304	1.742
F(000)	96	80
crystal dimensions (mm)	cylinder, ϕ 0.3	0.3 × 0.3 × 0.2
radiation	Mo Kα, Zr filter	Mo Kα, Zr filter
wavelength (λ (Å))	0.71068	0.71068
temp of measurement (K)	106 (1)	97 (1)
data collection range	4–115	4–110
(2θ, (deg)) (h, k, l)	h 0, 13	h −3, 10
	k 0, 15	k −12, 11
	l −14, 14	l −15, 13
standard reflections	−3, 3, 0; 1, 2, 2	1, 0, 4[a]
	−4, 0, 2; 1, 3, 1	0, −4, 0
	−1, 3, 3; 2, 2, −3	
	1, 1, 4; −1, 2, −2	
standard reflections when?	every 60 min	every 60 min
number of		
reflections collected	3893	4050
unique reflections	3044	3851
observed unique reflections	2272 ($F_o > 4\sigma(F_o)$)	3374 ($F_o > 2\sigma(F_o)$)
data collection instrument	SIEMENS four-circle diffractometer with quarter circle for χ and N_2 gas stream equipment	SIEMENS four-circle diffractometer with quarter circle for χ and N_2 gas stream equipment
orientation reflections (number, range (2θ, (deg)))	21, 26–30	23, 27–48[a]
scan method	Ω–2θ step scan, Ω steps 0.02°	Ω–2θ step scan, Ω steps 0.02°
scan width (deg)	$\Delta\Omega$ = 1.30 + 0.26 tan Ω	$\Delta\Omega$ = 1.70 + 0.26 tan Ω
scan rate (Ω (deg/min))	0.4–4.0	0.4–4.0
absorption correction	no	yes

[a] As soon as the intensity of any one of the standard reflections dropped by more than 3% with respect to the previous maximum value, the orientation reflections in the list were automatically recenterd, and a new orientation matrix was thereby determined. This happened about every 3–4 h.

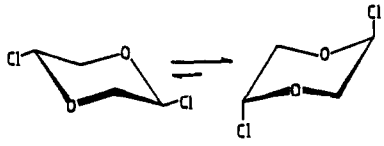

Figure 1. The anomeric effect: Electronegative substituents, attached to the anomeric carbon, prefer the axial setting, although from steric consideration alone the equatorial conformation would be favored.

Dichlorodioxane. DICLOX was synthesized by photochlorination of DIOX as described by Bryan, Smedley, and Summerbell.[12] Crystals were obtained by slow evaporation from a carbon tetrachloride solution. No phase transition was encountered during cooling. Crystal data and experimental details are given in Table I.

Theoretical Calculations. Ab initio calculations were carried out for DIOX, DICLOX, and difluorodioxane (DIFLOX) with the GAUSSIAN86[13] program package on a CRAY-XMP supercomputer. Several basis sets (3-21G, 6-21G, 4-31G*, and 6-31G*) have been tested. The first two gave little bond density, indicating the importance of the polarization functions, while the latter two resulted in similar deformation densities. The theoretical maps presented here are all calculated at the 6-31G* level. Geometrical parameters for DIOX and DICLOX were taken respectively from X-ray and neutron refinements. Parameters for DIFLOX were constructed from those of the chloro compound by shortening the carbon halogen bond to 1.367 Å.

Wave functions for the free atoms were calculated separately with the same basis set. The resulting atomic densities were spherically symmetrized and subtracted from the total density. Optimizations of the geometry of 1-chloroethanol and 2-chloroethyl methyl ether, as model fragments for DICLOX, were carried out using the GAUSSIAN ab initio program package. The highest basis set applied was 6-31G*. These optimizations gave only small shifts in the geometry of the fragments away from the experimental values. This indicates that the fragments provide a relatively good model for the whole molecule. Theoretical ab initio deformation density maps were calculated by Pichon-Pesme and Hansen[14] for dimethyl ether as well as for *gauche*- and *trans*-fluorodimethyl ether, taking the geometry from DICLOX. In the present work we report similar calculations for the whole molecules DIOX, DICLOX, and DIFLOX.

Refinement and Structure. The starting atomic coordinates were taken from previous structure determinations.[8,9] The conventional refinements were carried out with the SFLSX full-matrix least-squares program of the XTAL[15] system of crystallographic programs. Scattering factors, including those of anomalous scattering, were taken from the International Tables.[16] For hydrogen atoms the scattering factors given by Stewart et

(11) Luger, P. *KAPKOR. An endless cylinder volume correction program*; Freie Universität Berlin: Berlin, 1984; unpublished work.
(12) Bryan, L. A.; Smedley, W. M.; Summerbell, R. K. *J. Am. Chem. Soc.* **1950**, *72*, 2206.
(13) Gaussian 86: Frisch, M. J.; Binkley, J. S.; Schlegel, H. B.; Raghavachari, K.; Melius, C. F.; Martin, R. L.; Stewart, J. J. P.; Bobrowicz, F. W.; Rohlfing, S. M.; Kahn, L. R.; Defrees, D. J.; Seeger, R.; Whiteside, R. A.; Fox, D. J.; Fleuder, E. M.; Pople, J. A. Carnegie-Mellon Quantum Chemistry Publishing Unit: Pittsburgh, PA, 1984.
(14) Pichon-Pesme, V.; Hansen, N. K. *J. Mol. Struct*: THEOCHEM **1989**, *183*, 151–160.
(15) Hall, S. R., Stewart, J. M., Eds. *XTAL 2.2 Users Manual*; University of Western Australia: Nedlands, WA, University of Maryland: College Park, MD, 1987.
(16) Ibers, J. A., Hamilton, W. C. Eds. *International Tables for X-Ray Crystallography*; The Kynoch Press: Birmingham, England; Vol. IV.

Table II. Least-Squares Refinements

	DIOX		DICLOX	
	spherical atoms	multipole atoms	spherical atoms	multipole atoms
refinement based on	F	F	F	F
weight	$1/\sigma(F_o)$	$1/\sigma(F_o)$	$1/\sigma(F_o)$	$1/\sigma(F_o)$
σ cutoff	4σ	4σ	2σ	3σ
number of				
reflections n	2272	2272	3374	3295
variables m	44	52	50	130
extinction parameters			1	1
R^a	0.039	0.027	0.032	0.026
wR^b	0.042	0.024	0.030	0.021
S^c	2.60	1.55	2.54	1.74
$(\Delta/\sigma)_{max}$ in last cycle	0.08		0.10	

$^a R = \Sigma(||F_o| - |F_c||)/\Sigma|F_o|$. $^b wR = [\Sigma w(|F_o| - |F_c|)^2/\Sigma wF_o^2]^{1/2}$. $^c S = [\Sigma w(|F_o| - |F_c|)^2/(n-m)]^{1/2}$.

Table III. Atomic Parameters for Dioxane (U_{eq} and U in Å^{2}100)

atom	X	Y	Z	U_{eq} or U
O(1)	0.715 69 (4)	0.613 69 (4)	0.525 60 (5)	1.902 (6)
C(1)	0.500 42 (6)	0.706 63 (6)	0.567 63 (6)	1.825 (8)
C(2)	0.662 24 (6)	0.455 95 (6)	0.361 09 (6)	2.006 (8)
H(11)	0.425 (1)	0.775 (1)	0.430 (1)	2.4 (2)
H(12)	0.543 (1)	0.811 (1)	0.683 (1)	2.2 (1)
H(21)	0.589 (1)	0.516 (1)	0.223 (1)	2.3 (2)
H(22)	0.810 (1)	0.396 (1)	0.336 (1)	2.5 (2)

Table IV. Atomic Parameters for Dichlorodioxane (U_{eq} and U in Å^{2}100)

atom	X	Y	Z	U_{eq} or U
Cl(1)	0.230 12 (4)	0.248 48 (3)	0.154 15 (3)	1.705 (4)
O(1)	0.665 5 (1)	0.312 89 (9)	0.512 38 (7)	1.445 (9)
C(1)	0.593 9 (1)	0.443 0 (1)	0.325 97 (9)	1.37 (1)
C(2)	0.447 9 (2)	0.296 5 (1)	0.643 2 (1)	1.46 (1)
H(1)	0.753 (2)	0.459 (2)	0.247 (1)	1.0 (2)
H(21)	0.524 (2)	0.221 (2)	0.778 (2)	1.3 (2)
H(22)	0.244 (2)	0.187 (2)	0.580 (2)	1.5 (3)

Table V. Bond Distances (Å), Bond Angles (deg) and Torsion Angles (deg) in the Dioxane Molecule[a]

atom				distance	angle	torsion angle
A	B	C	D	B–C	A–B–C	A–B–C–D
C(2)′	C(1)	O(1)	C(2)	1.4315 (6)	110.49 (4)	57.2 (1)
				1.4286 (2)	110.62 (2)	57.2 (1)
C(1)	O(1)	C(2)	C(1)′	1.4294 (6)	109.84 (3)	−57.5 (1)
				1.4288 (6)	109.97 (1)	−57.4 (1)
O(1)	C(2)	C(1)′	O(1)′	1.5155 (6)	110.96 (4)	57.9 (2)
				1.5149 (2)	110.86 (2)	57.5 (1)
O(1)	C(1)	H(11)		0.983 (7)	107.5 (4)	
				1.066 (3)	108.5 (2)	
O(1)	C(1)	H(12)		0.974 (7)	107.6 (4)	
				1.044 (3)	107.1 (2)	
O(1)	C(2)	H(21)		0.962 (7)	109.9 (5)	
				1.052 (3)	109.2 (2)	
O(1)	C(2)	H(22)		0.967 (7)	108.0 (4)	
				1.049 (3)	105.9 (2)	
C(2)′	C(1)	H(11)			111.0 (4)	
					109.9 (2)	
C(2)′	C(1)	H(12)			111.0 (4)	
					111.7 (2)	
C(1)′	C(2)	H(21)			109.9 (4)	
					109.4 (2)	
C(1)′	C(2)	H(22)			111.5 (4)	
					111.5 (2)	
H(11)	C(1)	H(12)			109.1 (6)	
					109.0 (4)	
H(21)	C(2)	H(22)			106.5 (6)	
					109.9 (4)	

[a] Entry in upper line is X-ray data and conventional refinement, in lower line X-ray data and multipole refinement.

al.[17] were used. Details of the refinements are given in Table II. The quantity minimized was $\sum w(|F_o| - |F_c|)^2$.

Table VI. Bond Distances (Å), Bond Angles (deg), and Torsion Angles (deg) in the Dichlorodioxane Molecule[a]

atom				distance	angle	torsion angle
A	B	C	D	B–C	A–B–C	A–B–C–D
C(2)′	C(1)	O(1)	C(2)	1.3832 (8)	112.81 (6)	51.81 (6)
				1.3843 (6)	112.61 (7)	51.94 (2)
				1.3815 (6)	112.66 (4)	51.85 (4)
C(1)	O(1)	C(2)	C(1)′	1.433 (1)	113.20 (6)	−51.31 (7)
				1.4292 (7)	113.48 (4)	−51.44 (3)
				1.4294 (8)	113.41 (4)	−51.36 (5)
O(1)	C(2)	C(1)′	O(1)′	1.511 (1)	111.78 (6)	51.07 (7)
				1.5157 (7)	111.65 (3)	50.98 (4)
				1.5134 (8)	111.72 (4)	50.97 (5)
H(1)	C(1)	Cl(1)		1.8421 (7)	102.9 (5)	
				1.8434 (6)	104.73 (5)	
				1.8419 (6)	104.65 (6)	
Cl(1)	C(1)	O(1)	C(2)		110.14 (4)	−70.63 (6)
					110.24 (3)	−70.48 (5)
					110.25 (3)	−70.53 (5)
Cl(1)	C(1)	C(2)′	O(1)′		109.32 (5)	71.83 (6)
					109.35 (3)	71.94 (4)
					109.29 (4)	71.95 (5)
O(1)	C(1)	H(1)		0.96 (1)	110.4 (6)	
				1.092 (1)	107.92 (6)	
				1.093 (1)	107.95 (6)	
C(2)′	C(1)	H(1)			110.8 (6)	
					111.70 (5)	
					111.75 (6)	
O(1)	C(2)	H(21)		0.97 (1)	109.5 (7)	
				1.092 (1)	106.73 (7)	
				1.093 (1)	106.68 (7)	
O(1)	C(2)	H(22)		0.958 (9)	109.7 (7)	
				1.099 (1)	109.82 (7)	
				1.099 (1)	109.84 (7)	
C(1)′	C(2)	H(21)			110.0 (7)	
					111.48 (6)	
					111.58 (6)	
C(1)′	C(2)	H(22)			107.7 (7)	
					107.71 (7)	
					107.72 (7)	
H(21)	C(2)	H(22)			108.0 (8)	
					109.45 (7)	
					109.27 (7)	

[a] Entry in upper line is X-ray data and conventional refinement, in middle line neutron data, and in lower line X-ray data and multipole refinement.

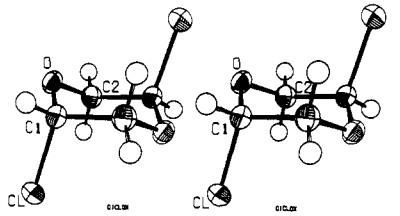

Figure 2. Stereo ORTEP drawing of the DICLOX molecule; ellipsoids at the 80% probability level.

The data for DICLOX were corrected for both absorption and extinction. The presence of extinction was discovered by ψ scans on a few reflections. The mean path lengths were obtained by the program ABSORB of the XTAL system. Extinction effects were significant, and an isotropic extinction parameter was included in the XTAL refinement calculations. The reflections most severely affected were −1, 1, 0; −1, 0, 1; and 1, 1, 1, with $0.95F_c$. The atomic parameters for DIOX and for DICLOX are listed in Tables III and IV, respectively. The geometrical parameters are in Tables V and VI. These values are in good agreement with the results of a single-crystal neutron diffraction experiment on DICLOX described elsewhere.[18] Figure 2 shows an ORTEP plot of the DICLOX molecule. The variation in the structural parameters is only small in comparison to the previous investigations. As expected, the two C–O bonds are almost equal, 1.4315 (6) and 1.4291 (6) Å in DIOX, and

(17) Stewart, R. F.; Davidson, E. R.; Simpson, W. T. *J. Chem. Phys.* **1965**, *42*, 3175–3187.

(18) Jeffrey, G. A.; McMullan, R. K.; Ruble, J. R.; Buschmann, J.; Luger, P. *Acta Crystallogr., Sect. C*, in press.

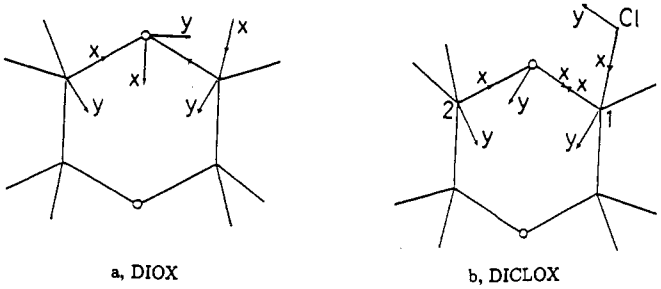

Figure 3. Coordinate systems used for the individual atoms in multipole calculations: (a) for dioxane; (b) for dichlorodioxane.

Table VII. Significant Multipole Populations for Dioxane ($P_{lm} \geq 2\sigma(P_{lm})$)

		atom		
		O	C	
l	m	(mm2 symm)	(m symm)	H
0	0	6.19 (5)	4.10 (4)	0.90 (6)
1	1	−0.08	−0.05	0.13
1	−1		−0.04	
2	0	0.09	0.03	
2	2	0.08	−0.05	
2	−2		0.00	
3	1	−0.04	−0.17	
3	−1		−0.18	
3	3	−0.07	0.23	
3	−3		0.05	
4	0	0.00	0.05	
4	2	0.03	−0.04	
4	−2		0.11	
4	4	−0.02	0.07	
4	−4		0.04	

very close to the C–O bond not containing the anomeric carbon in DICLOX which is 1.433 (1) Å. The anomeric C–O bond in the latter compound is 1.3832 (8) Å, a significant shortening compared to the above values. A C–Cl bond length is 1.8421 (7) Å, in close agreement with other anomeric C–Cl bond distances as mentioned in the Introduction. The C–O–C angle is 109.90 (3)° and 113.20 (6)° in DIOX and DICLOX, respectively. The widening of this angle is also in accord with the anomeric effect.

Multipole Refinement. The program system MOLLY[19] was used for the multipole refinement, where the aspherical atomic density $\rho(r)$ is described in terms of spherical harmonic expansion:

$$\rho(\vec{r}) = P_c\rho_c(r) + P_v\kappa^3\rho_v(\kappa r) + \sum_{l=0}^{4} R_l(\kappa' r) \sum_{m=-l}^{l} P_{lm} Y_{lm}(\vec{r}/r)$$

where ρ_c and ρ_v are the spherical Hartree–Fock core and valence densities, R_l and Y_{lm} stand for radial and real, normalized angular functions, respectively. Beside the conventional crystallographic parameters, the P_c, P_v and P_{lm} populations and the expansion–contraction variables κ and κ' can be refined. The Fourier–Bessel transforms $\langle J_0 \rangle$ of ρ_c and ρ_v are given in the International Tables,[16] and for the R_l radial functions the standard, optimized Slater orbitals were taken.[20] For the carbon atoms of DIOX the valence deformations were constrained to be equal. Similar constraints were used for the hydrogen atoms in both molecules. In the local coordinate systems, illustrated in Figure 3a,b, mm2 and m site symmetries were assumed for the O and C atoms, respectively, in the unsubstituted dioxane ring. In the chlorinated molecule these symmetry restraints were not applied, only an m symmetry to the unsubstituted carbon atom.

For both molecules the non-hydrogen atoms were treated up to the hexadecapolar level in the multipole expansion. The charge density asphericity for all H atoms was represented by a common dipole along the C–H bond. In the case of the DICLOX molecule the positional and thermal parameters of the hydrogens were fixed at the values obtained from the neutron measurement.

The aspherical refinement gave improved agreement with reduced esd's in comparison to the conventional fit. Details of the multipole refinements are given in Table II. The final populations for both molecules are listed in Tables VII and VIII. The κ values for the results

Table VIII. Significant Multipole Populations for Dichlorodioxane ($P_{lm} \geq 2\sigma(P_{lm})$)

		atom				
					C(2)	
l	m	Cl(1)	O(1)	C(1)	(m symm)	H
0	0	7.01 (5)	6.09 (5)	4.06 (4)	4.18 (4)	0.89 (6)
1	1	−0.05	−0.06	−0.06	−0.08	0.11
1	−1	0.00	−0.09	0.00	−0.11	
1	0	−0.02	0.00	−0.07		
2	0	−0.12	0.11	−0.03	0.06	
2	1	−0.08	0.07	0.17		
2	−1	−0.26	−0.03	0.10		
2	2	−0.26	0.00	0.00	−0.03	
2	−2	−0.22	−0.07	−0.04	0.07	
3	0	0.03	−0.02	0.03		
3	1	−0.04	−0.05	−0.15	−0.20	
3	−1	0.00	−0.01	−0.21	−0.18	
3	2	0.00	−0.02	−0.03		
3	−2	0.02	0.00	−0.07		
3	3	0.03	0.04	0.21	0.22	
3	−3	0.02	0.00	0.05	0.05	
4	0	0.00		0.05	0.06	
4	1	0.00	0.00	−0.03		
4	−1	−0.14	0.02	0.04		
4	2	0.17	0.03	−0.08	−0.05	
4	−2	−0.02	0.00	0.10	0.09	
4	3	0.11	0.09	−0.04		
4	−3	0.00	−0.04	0.12		
4	4	0.03	0.04	0.08	0.07	
4	−4	0.05	0.04	0.03	0.04	

Table IX. Rigid-Body Motion Analysis

	eigenvector			eigenvalue (Å², deg²)	residual[a]
		DIOX Multipole Refinement			
	−0.4560	−0.8647	0.2107	0.0161	
T	0.7873	−0.5023	−0.3575	0.0140	
	0.4149	0.0028	0.9098	0.0098	
					0.009
	0.7427	0.6690	−0.0279	23.55	
L	−0.6625	0.7283	−0.1752	15.63	
	−0.0969	0.1486	0.9841	4.88	
		DICLOX Neutron Refinement			
	0.8060	0.4076	−0.4292	0.0105	
T	−0.5808	0.6846	−0.4405	0.0091	
	0.1143	0.6043	0.7885	0.0081	
					0.023
	0.9666	0.0006	−0.2562	8.10	
L	0.0366	0.9894	0.1403	3.79	
	0.2535	−0.1450	0.9564	2.43	
		DICLOX Multipole Refinement			
	0.8233	0.3602	−0.4386	0.0132	
T	−0.5673	0.4974	−0.6564	0.0114	
	−0.0183	0.7892	0.6139	0.0099	
					0.026
	0.9419	0.1044	−0.3193	8.34	
L	−0.0409	0.9790	0.1996	4.08	
	0.3335	−0.1749	0.9264	2.17	

[a] $R = \Sigma w(U^o_{ij} - U^c_{ij})^2 / \Sigma w U^o_{ij}{}^2$.

presented here are all equal to unity.

Thermal Motion Analysis. Rigid-body motion analysis of the atomic vibration tensors was carried out by the method of Schomaker and Trueblood[21] with the aid of the THMA11 computer program. The thermal parameters obtained from the multipole refinement on X-ray data for both compounds were tested. In all cases the H atoms were not included in the calculation. Table IX summarizes the results in terms of the eigenvectors and eigenvalues of the translation (T) and libration (L) tensors in the molecular inertial system. The agreement between the observed and calculated U_{ij} values is good, which indicates that the internal modes make only a minor contribution to the atomic displacements. The X-ray and neutron results for DICLOX are in good agreement; the differences between them are accounted for by the translational

(19) Hansen, N. K.; Coppens, P. *Acta Crystallogr.* **1978**, *A34*, 909–921.
(20) Clementi, E.; Raimondi, D. L. *J. Chem. Phys.* **1963**, *38*, 2686–2689.
(21) Schomaker, V.; Trueblood, K. N. *Acta Crystallogr.* **1968**, *B24*, 63–76.

components of the rigid-body motion. In addition, the rigid-bond criterion[22] is equally well satisfied. The differences in the bond components of the U_{ij}'s for the connected atom pairs are in the range of (3–4) × 10^{-4} Å^2 for both observations.

Experimental Electron Deformation Density. Electron density deformations due to chemical bonding are usually represented in terms of difference density maps, i.e., as the difference between the actual electron density in the crystal and the superimposed spherical free atom densities centered at the observed nuclear positions (promolecule). Dynamic electron deformation density maps (DDD) are calculated by the usual difference Fourier syntheses of the type

$$\Delta\rho(r) = (2/V)\sum_{\mathbf{H}}\Delta F(\mathbf{H})\exp(-2\pi i\mathbf{H}r)$$

The Fourier coefficients ΔF are given by

$$\Delta F(\mathbf{H}) = F_o(\mathbf{H}) - F_{c\,sph}(\mathbf{H})$$

where F_o are the observed and $F_{c\,sph}$ the conventionally calculated structure factors. The atomic parameters for $F_{c\,sph}$ were obtained from multipole refinement for DIOX and from the neutron diffraction experiment for DICLOX. The atomic temperature factors from the neutron measurement were scaled up to the X-ray parameter level by an overall isotropic correction term fitted to the X-ray data ($\exp(-8\pi^2u_o\sin^2\Theta/\lambda^2)$ where u_o = 0.00234 Å^2). During the refinement of this parameter the atomic positions were fixed at their neutron values.

To filter the experimental noise due to the lower statistical accuracy of the high-angle Bragg reflections, only the low-order data ($\sin\Theta/\lambda \leq 0.85$ Å^{-3}) with $|F_o| \geq 3\sigma(|F_o|)$ were included in the Fourier summation. For the presented sections of the DDD maps the standard deviation is estimated to be smaller than 0.05 e/Å^3 for a general position.

The static deformation density (SDD) is calculated from the refined parameters of the multipole model. In this formalism the thermal smearing of the charge density due to atomic vibrations can be deconvoluted; thus, the obtained ED can directly be compared to the theoretical maps. In all of the presented sections, the contour intervals are 0.1 e/Å^3.

The construction of a promolecule usually includes some arbitrariness in the choice of the proper atomic ground state. In order to obtain spherically averaged atomic densities, the electrons are equally shared among atomic orbitals. Thus, the spherical model usually assumes more than one electron for the orbital forming the bond and less than two for the nonbonded orbitals. As a result the conventional EDD may not show the expected bond peaks and extra charge accumulation may appear in the nonbonded areas.[23,24] In order to overcome this problem, the oriented atom model was proposed by Schwarz et al.,[25] in which case the atoms are set up in the chemically expected hybridization. This method was shown to be useful in mapping charge accumulation along bonds to atoms of high valency,[26] but its applicability is not as straightforward for nontrivial hybridization.[27]

The ED of a fragment is transferable to a certain extent; i.e., it has local characteristics which are mostly independent of the neighboring atoms. Conversely, if the electronic properties of a group do not show the expected transferability, then the changes in the ED can directly be attributed to a different chemical environment. A straightforward way to demonstrate the fragment–fragment interaction is to compare the ED of the total system to the superimposed ED's of the free subsystems. Such a fragment deformation density (FDD) has proven its efficiency to demonstrate substituent effects[28] or structural changes.[29] This treatment assumes a partitioning of the molecular ED into fragment contributions. The multipole model, as a one-center representation of the molecular ED, implicitly involves atomic partitioning. Consequently, one can construct a promolecule or profragment from the "pseudoatoms" obtained after a multipole refinement. In the present study, we found it especially informative to interpret our results for DICLOX in terms of FDD, where the multipole ED obtained for DIOX provided the reference density. This representation avoids the above-mentioned difficulties in composing the promolecule of spherical atoms and provides a direct mapping of the changes in the ring's ED. An exception is the chlorine atom for which the artifacts of the spherical atom subtraction stay in effect.

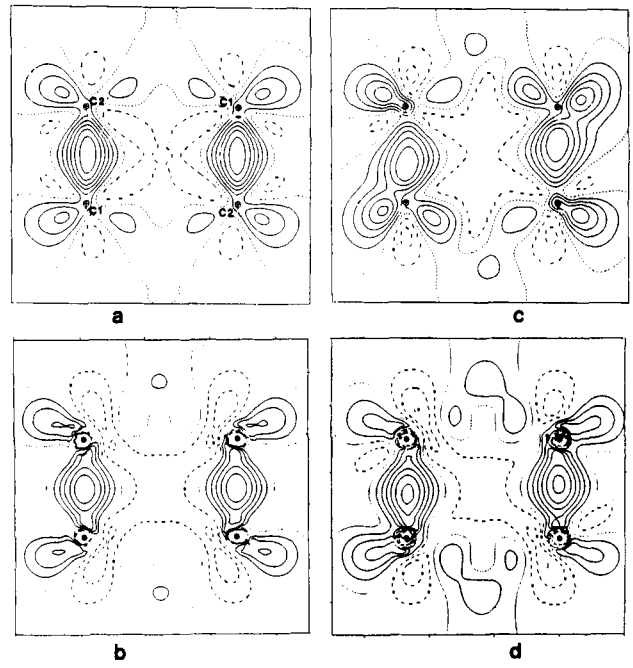

Figure 4. Section through the electron deformation density containing four carbon atoms: (a,b) dioxane; (c,d) dichlorodioxane; (a) experimental multipole; (b) theoretical; (c) experimental multipole; (d) theoretical.

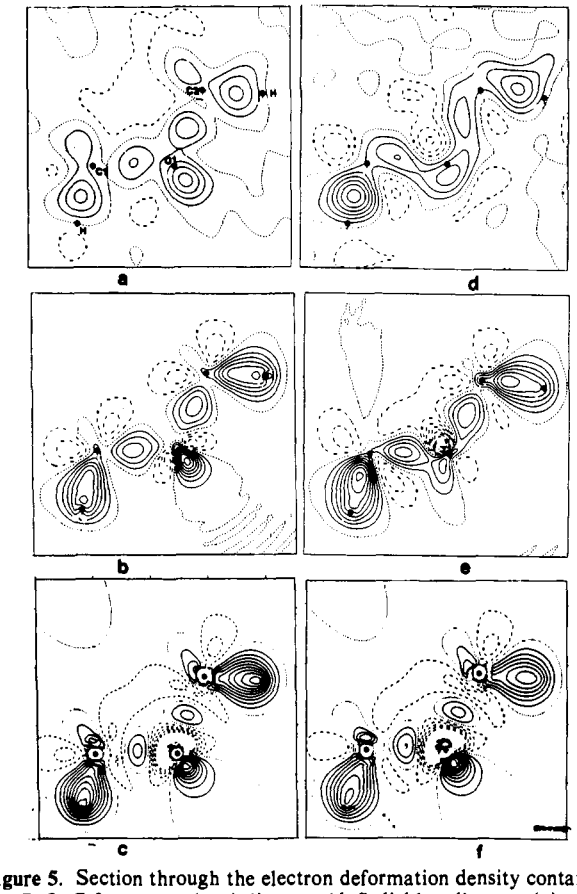

Figure 5. Section through the electron deformation density containing the C–O–C fragment: (a–c) dioxane; (d–f) dichlorodioxane; (a) experimental dynamic; (b) experimental multipole; (c) theoretical; (d) experimental dynamic; (e) experimental multipole; (f) theoretical.

Discussion

In order to examine the changes in the electronic state of the ring, due to the substitution, theoretical and experimental EDD's in several sections through both molecules were calculated and compared. In the following, experimental EDD refers to multipole

(22) Hirshfeld, F. L. *Acta Crystallogr.* **1976**, *A32*, 239.
(23) Dunitz, J. D.; Schweizer, W. B.; Seiler, P. *Helv. Chim. Acta* **1983**, *66*, 123–133.
(24) Seiler, P.; Schweizer, W. B.; Dunitz, J. D. *Acta Crystallogr.* **1984**, *B40*, 319–327.
(25) Schwarz, W. H. E.; Valtazanos, P.; Ruedenberg, K. *Theor. Chim. Acta* **1985**, *68*, 471–506.
(26) Takazawa, H.; Ohrba, S.; Saito, Y. *Acta Crystallogr.* **1989**, *B45*, 432–437.
(27) Buschmann, J.; Koritsanszky, T.; Luger, P.; Seppelt, A. *J. Am. Chem. Soc.* **1991**, *113*, 223–238.
(28) Eisenstein, M.; Hirshfeld, F. L. *J. Comput. Chem.* **1983**, *4*, 15.
(29) Nakatsuji, H. *J. Am. Chem. Soc.* **1973**, *95*, 2084.

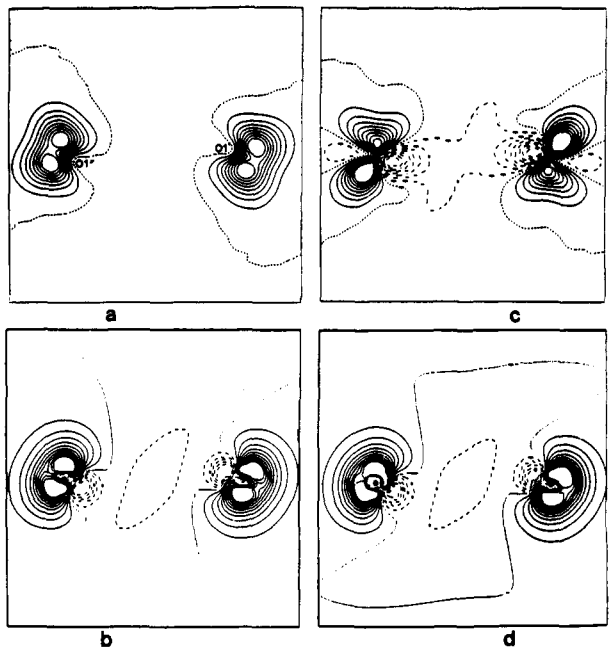

Figure 6. Electron deformation density containing the two oxygen atoms in a cut perpendicular to the ring: (a,b) dioxane; (b,c) dichlorodioxane; (a) experimental multipole; (b) theoretical; (c) experimental multipole; (d) theoretical.

deformation density. Although for DIOX the theory and the experiment give an extremely good agreement, some of the relevant deformations caused by the substitution of the chlorine atom can only be observed on the experimental maps.

Figure 4a–d shows the deformation densities around the four ring carbons that lie in a plane. In comparison to the free ring, a significant deviation appears at the substituted carbon (Cl and Cl′), where an extra charge accumulation is observable. As a result the C–C and C–H bond densities overlap and the maximum on the C–C bond peak shifts toward the anomeric carbon.

In Figure 5a–f static and theoretical maps in the C–O–C plane for both molecules are displayed. In DICLOX the substituted carbon forms a shorter bond with higher density than the unsubstituted one. The experimental maps for DICLOX (Figure 5d,e) show continuous density connecting the C–O bond with the nonbonded region of the oxygen. This charge migration leaves a depleted area in the inner side of the C–O–C bisector.

Figure 6a–d shows a plane that bisects the two C–O–C angles and thereby contains only the two oxygen atoms and their lone pair regions. Usual interpretations for these are derived from the $sp^2(n_\sigma)$, $p_z(n_\pi)$ or sp^3 hybridization whose maxima all fall onto the plane considered and are contained in a kidney-shaped density.[30] For DICLOX the theoretical map resembles closely the map of the unsubstituted molecule but the experiment gives the "rabbit ears" instead of the "kidney" shape (Figure 6c). The lobes are separated by a region of negative density which can be assigned to a missing n_σ contribution.

The O–C–Cl plane (Figure 7a–e) is of special interest, on which another view of the anomeric C–O bond is visible. For DICLOX the experiment, in contrast to the theory, indicates again the fusion of the oxygen lone pair and the C–O bond densities. Furthermore, an extended and pronounced charge accumulation is seen in the nonbonded area of the Cl atom at the expense of charge in the C–Cl bond direction. This feature is typical and can usually be attributed to the subtraction of a spherical atom. On Figure 7c the lone pair of the chlorine atom is not perpendicular to the bond; therefore, in this case the use of a normally oriented reference atom (in the P_x^1,S^2,P_y^2,P_z^2 configuration with the x direction along the bond) would not give the expected character to the charge deformation.

(30) Csizmadia, Ed. *Progress in Theoretical Organic Chemistry*; Elsevier: New York, 1977; Vol. 2.

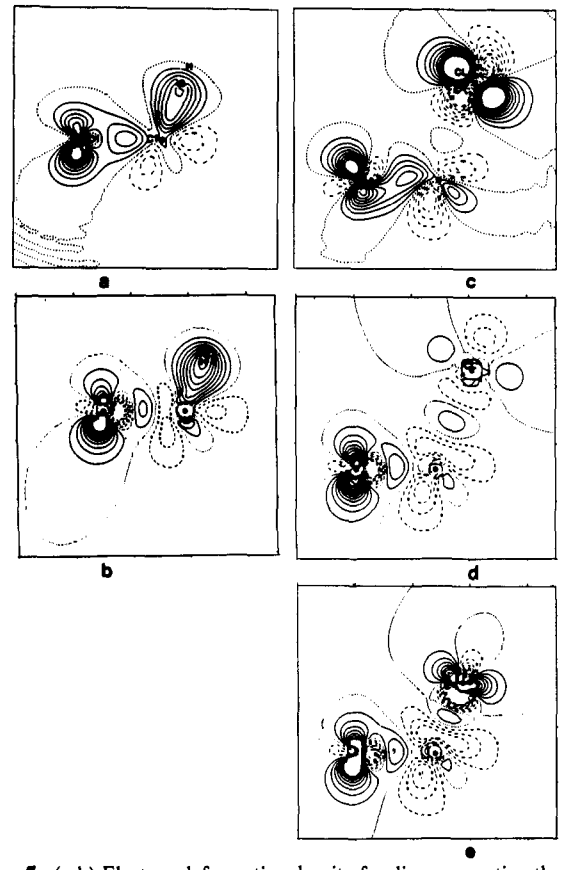

Figure 7. (a,b) Electron deformation density for dioxane; section through O–C–H(axial): (a) experimental multipole; (b) theoretical. (c,d) Electron deformation density for dichlorodioxane, O–C–Cl plane: (c) experimental multipole refinement; (d) theoretical; (e) theoretical map for difluorodioxane O–C–F plane.

The theory, in contrast to the experiment, gives weaker lone pair density which is perpendicular to the bond (Figure 7d). To further investigate this lack of density, a theoretical map for DIFLOX was also calculated using the same quality basis set (Figure 7e). Here the lone pair region is still perpendicular to the bond, but in size it already resembles the experimental map. In addition the electron-deficient regions along the bond are also reproduced. This comparison may indicate that the weak appearance of the nonbonded deformation around the Cl atom is due to a basis set effect in the calculation.

To test the significance of the experimentally observed lone pair inclinations, additional multipole refinements were carried out. First the C–Cl bond was constrained to have cylindrical symmetry. Much worse residuals resulted and the esd's for the multipole populations of the Cl atom increased to an extent that cannot be attributed to the decrease in the refinable variables.

Further attempts to keep the mm or m site symmetry of the oxygen atom in DICLOX during the multipole refinement also failed. On the other hand, an attempted unconstrained refinement on the DIOX data set without the assumed mm2 site symmetry for the oxygen atom did not result in significant populations of the symmetry-released spherical harmonics.

Figure 8a–c displays FDD's in the three planes which are discussed above. The FDD is defined as

$$\rho_{FDD} = \rho_{mul}(DICLOX) - [\rho^0_{mul}(DIOX) + \rho_{sph}(Cl)]$$

where $\rho^0_{mul}(DIOX)$ is composed of the refined pseudoatoms which are placed at the corresponding position to reproduce the molecular structure of DICLOX. Then the FDD can be calculated either by subtracting the numerical values of the profragment ED at each grid point from the ED of DICLOX or directly from the difference of the multipole populations transformed to the same local coordinate system. Hydrogen atoms are not included, and for the chlorine atom spherical density is subtracted. Since the

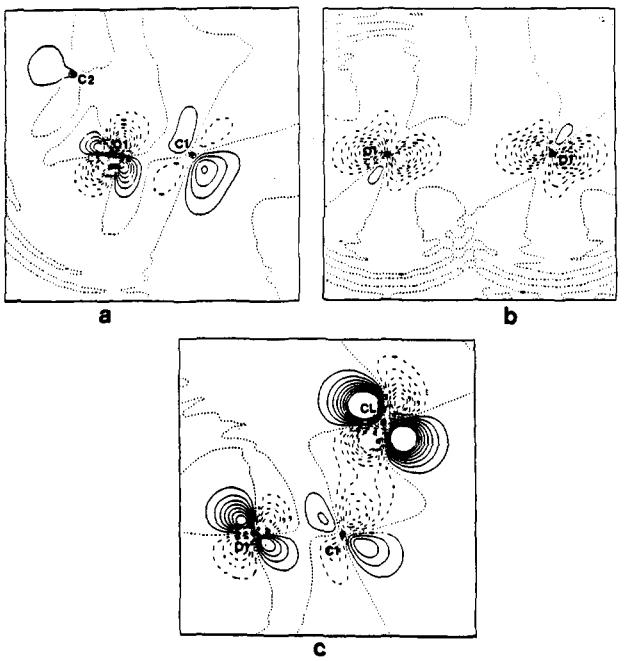

Figure 8. Fragment deformation density map prepared by subtracting the individual atomic densities of dioxane from the corresponding densities in dichlorodioxane. Sections illustrated: (a) C–O–C plane; (b) plane perpendicular to the ring and containing the two oxygens; (c) O–C–Cl plane.

net atomic charges for the two molecules are very close in value, only minor monopole contributions occur on these maps.

The C–O–C plane (Figure 8a) shows well-defined parallel quadrupoles at the oxygen and at the substituted carbon atom. The negative lobes for the oxygen are situated nearly on the bisector of the C–O–C angle. Negligible density is localized on the methylene carbon, indicating that the substitution has no effect on this atom.

The O–C–Cl section of the FDD (Figure 8c) presents quite similar valence asphericities where the positive and negative lobes are again pairwise parallel. In any parallel cuts through the three atoms the FDD exhibits topological equivalence, indicating that the nonbonded peaks are strongly correlated regarding their expansion and orientation.

The directional characteristic of the FDD shows that, due to the substitution, a considerable change occurred in the mixing of the oxygen atom's p orbitals. It is important to note that the main contribution to the deformations is the $p_x p_y$ term formed by the σ p orbitals (C–O–C plane) that are involved in bonding and in forming the nonbonded $n_\sigma(O)$ and not the $n_\pi(O)$ usually attributed to the anomeric effect.

Conclusion

The following qualitative statements are based on the observed characteristics of the FDD.

(1) The density deformation caused by the substitution is localized on the first (C) and second (O) neighbor atoms to the chlorine.

(2) The quadrupolar character of the deformation indicates that the charge rearrangement is mainly due to the change in the p–p-type orbital mixing; hence, at the O and Cl atoms the lone pair orbitals must be effected.

(3) The correlated orientation of the lobes at the O, C, and Cl atoms and the deformation on the anomeric carbon suggest the presence of three-center interactions which take place through the O–C and C–Cl bonds.

(4) The deformation at the Cl atom may imply that the $n_\pi(Cl)$ orbitals are also involved in the bonding system. Since the chlorine atom is bound to an asymmetric carbon, the C–Cl fragment has no rotational symmetry. In this case the $n_\pi(Cl)$ orbitals are not necessarily equivalent and must not necessarily occupy any mutually orthogonal directions. The splitting of the equivalent π orbitals can be accompanied by a mixing of the "coaxial" $n_\sigma(Cl)$ and the lower of the $n_\pi(Cl)$ orbitals. As a result, neither are the $n_\pi(Cl)$ orbitals perpendicular to nor is the $n_\sigma(Cl)$ collinear with the C–Cl bond.

(5) The charge rearrangement found at the chlorine is analogous to that observed at the O atom, but here the σ component is the dominant contribution in the density deformation, whereby a decrease of the $n_\sigma(O)$ density is observed in the C–O–C plane. Symmetry considerations dictate the presence of the $n_\sigma(O)$–σ^*(C–H) coupling, but it is less favored energetically when the $n_\pi(O)$–σ^*(C–Cl) coupling. In addition, this interaction would result in a lengthening of the C–H bond to the anomeric carbon, but it is not supported by the neutron data.

Summarizing, the FDD provides evidence for the mixing of lone pair orbitals at both ends of the O–C–Cl skeleton. The observed charge shifts at the terminal atom seem to be more complex than what could be directly attributed to the interaction of partially occupied nonbonded antibonding molecular orbitals. We cannot attribute the observed rearrangement to a π back-bonding, which is supposed to account for the anomeric phenomenon, and which might have only a secondary effect on the charge density.

To find out more about the importance of the $n_\pi(O)$–σ^*(C–Cl) overlap in stabilizing the axial conformer, the ED of the corresponding equatorial compound should also be examined.

Acknowledgment. This work was funded by a grant of the Federal Minister for Research and Technology (BMFT), under Contract No. PFR-AN204-03B72A460, by the Deutsche Forschungsgemeinschaft (DFG) and by the Fonds der Chemischen Industrie.

Registry No. DIOX, 123-91-1; DICLOX, 7429-31-4; DIFLOX, 136476-31-8.

Supplementary Material Available: Tables of atomic positional and anisotropic thermal parameters and bond lengths and angles (6 pages); lists of observed and calculated structure factors (63 pages). Ordering information is given on any current masthead page.